NJC

Accepted Manuscript

This article can be cited before page numbers have been issued, to do this please use: J. Qi, K. Qian, L. Tian, Z. Cheng and Y. Wang, *New J. Chem.*, 2018, DOI: 10.1039/C8NJ00697K.

ROYAL SOCIETY OF CHEMISTRY

rsc.li/njc

View Article Online
DOI: 10.1039/C8NJ00697K

New Journal of Chemistry

ARTICLE

Gallium(III)-2-benzoylpyridine-thiosemicarbazone complexes promote apoptosis through Ca^{2+} signaling and ROS-mediated mitochondrial pathways

Received 00th January 20xx,
Accepted 00th January 20xx

DOI: 10.1039/x0xx00000x

www.rsc.org/

Jinxu Qi,[a] Kun Qian,[a] Liang Tian,[a] Zhen Cheng [b] and Yihong Wang [*a]

Ga(III) compounds are highly promising candidates for antitumor therapy. The level of intracellular reactive oxygen species (ROS) is significantly increased after Ga(III) complexes treatment, but these complexes are redox-inactive. To investigate the effects of Ga(III) complexes on ROS levels, we synthesized three bis-ligated gallium(III)-2-benzoylpyridine-thiosemicarbazone complexes and studied their antitumor mechanisms. The structures of the Ga(III) complexes were identified by X−ray single-crystal diffraction. Cytotoxicity analysis demonstrated that ligands and gallium complexes exerted a higher antitumor activity and lower cytotoxicity than those of normal cells. The most active complex was C3, which exhibited a better antitumor viability than its related ligands and the anticancer agent 3−AP. Thus, Ga(III) complexes not only transmitted the iron ions but also induced intracellular Ca^{2+} release. As a result, the ROS standards in redox-active iron complexes were increased. The mechanism involved the release of Cyt C from the mitochondria which lack membrane potential, and then activation of the Caspase family proteins stimulated cell apoptosis.

Introduction

Gallium(III) nitrate is a first-generation gallium compound for therapeutic use and shows substantial selectivity to malignant tumors.[1-3] This selectivity is probably due to the similar chemical properties with iron that enables gallium to interfere with the intracellular iron metabolism.[4] A consequence of gallium-induced cellular iron dissipation is the inhibition of iron-containing protein activity.[5,6] Gallium nitrate, gallium tris−maltolate and gallium tris−8−quinolinolate (KP46) (Scheme 1) have been studied in preclinical and clinical trials and exerted considerable therapeutic effects various solid tumours.[7,8] However, the poor bioavailability and antitumor activity limit the development of gallium compounds.[9] The coordination of gallium(III) and ligands can improve the compounds' anticancer activity by increasing their lipophilicity and preventing hydrolysis.[4, 10] Recent studies have demonstrated that gallium complexes promote apoptosis through the mitochondrial signaling pathway under the regulation of the Bcl-2 family proteins.[4, 11] In clinical practice, $Ga(NO_3)_3$ is combined with hydroxyurea, mitoguazone or etoposide to achieve a good therapeutic effect.[12, 13]

Disrupting iron ion metabolism is an antiproliferative mechanism of thiosemicarbazone chelators, which are similar to gallium(III) nitrate.[14, 15] 3−Aminopyridine−2−carboxylaldehyde thiosemicarbazone (3−AP) (Scheme 1), an agent in phase II trials for treating various kinds of cancers, is the most outstanding anticancer agent among many thiosemicarbazone chelator derivatives.[16] Further studies showed that the [C1=NNH(CS)N4] is the basic structural unit of thiosemicarbazone compounds for biological activity.[17-19] Through their N and S atoms, thiosemicarbazone compounds easily form stable complexes with various of metal ions.[20, 21] Many reports proposed that thiosemicarbazone−metal complexes manifest a markedly higher antiproliferative activity than that of their corresponding ligands.[22-27] Richardson's results showed that the Ni(II), Zn(II), and Mn(II) thiosemicarbazide analogy complexes display similar antitumor activities to those of their ligands.[28] Generally, the gallium(III) complexes show increased anticancer activity relative to those of their corresponding ligands, whereas iron(III) coordinations' antitumor activity is substantially decreased with respect the corresponding ligands.[27, 29]

The treatment of lung cancer has greatly progressed in recent years, but numerous of patients die of this cancer every year.[30] Therefore, the development of new anticancer drugs is particularly urgent. Considering that thiosemicarbazone compounds show significant anticancer activity and potential medicinal value, we performed the following experiments in this study: (1) synthesis and characterization of the crystal structure of three 2:1 ligand/Ga (III) complexes by X−ray (Scheme 1), (2) assay of the electrochemical properties of Ga (III)/Fe(III) complexes by Cyclic Voltammetry, (3)

[a] School of Chemistry and Chemical Engineering, Southeast University, Nanjing 211189, China.
[b] Stanford Cancer Institute, Member of Academic Council, Stanford University, USA.

† Footnotes relating to the title and/or authors should appear here.
Electronic Supplementary Information (ESI) available: [details of any supplementary information available should be included here]. See DOI: 10.1039/x0xx00000x

View Article Online
DOI: 10.1039/C8NJ00697K

determination of the Ga (III) complexes' anticancer activity in a series of cancerous cell lines, and (4) investigation of the potential mechanism of NCI-H460 human lung cancer cell apoptosis induced by the Ga (III) complexes.

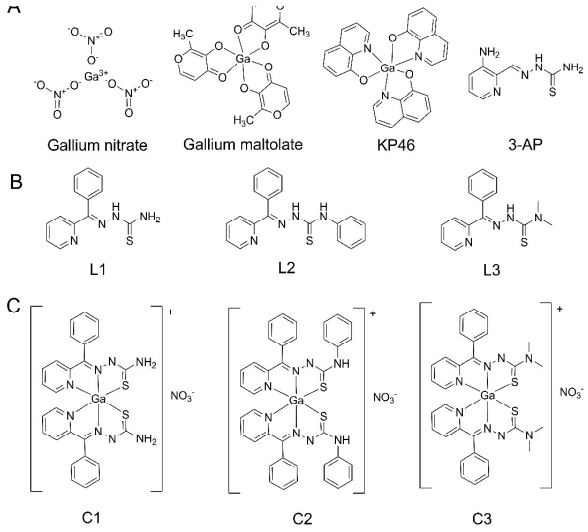

Scheme 1. (A) Chemical structures of gallium compounds and 3-AP currently in use in the clinic; (B) 2-benzoylpyridine-thiosemicarbazone ligands; (C) Gallium(III)-2-benzoylpyridine-thiosemicarbazones complexes.

Results and discussion

Synthesis of Ga(III) complexes.

Ligands L1-L3 were prepared straightforwardly via Schiff base condensation reactions. The synthesis reactions of the Ga(III) complexes were similar to one another. The methyl alcohol solution of $Ga(NO_3)_3$ was added into the solution of the ligands in methyl alcohol with stirring. The single crystals of Ga(III) complexes suitable for X-ray diffraction were crystallized from the solution in several days.

Crystal structure description.

The structures of three Ga(III) complexes (C1, C2 and C3) have been identified by X−ray (Fig.1). The crystal data of C1, C2 and C3 are shown in Tables S1 and Table S2. Crystal structure showed that these Ga (III) complexes were similar in coordination mode. The single-crystal X-ray diffraction structural analysis had revealed that C1 crystallized in the monoclinic with space group $P2_1/c$, C2 crystallized in the triclinic with space group P-1, and C3 crystallized in a monoclinic system with space group $P2_1/n$. The coordination environment of Ga(III) is contented by a pyridyl ring and thioamide tautomer form ligands. Two ligands were present in each Ga(III) complex molecule, and a pair of coordination atoms (N1/N2/S1 and N5/N6/S2) were both in a plane, respectively. The Ga(III) metal center was coordinated by four N atoms (N1, N2, N5 and N6) and two S atoms (S1 and S2) from two Schiff base ligands, leading to a deformation of octahedral configuration. The C=N double bond of the thioamide tautomer separated the ligand into 2-penzoylpyridine and thiosemicarbazone. The bond length of Ga–N (2.036−2.107 Å) and Ga–S (2.336–2.373 Å) were comparable to analogous distances in other known complexes. [4, 31, 32] Moreover, the distances of C–S bond (1.731–1.737 Å) in all complexes were similar to a single bond distance (ca. 1.81 Å) and double bond

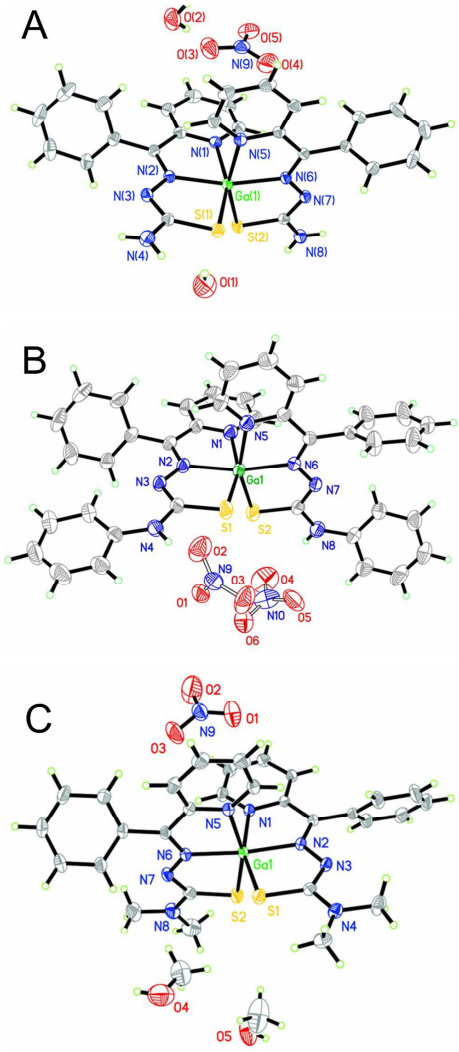

Fig. 1. The molecular structure of C1 (A), C2 (B) and C3 (C) showing the environment about the Ga(III) atom.

(ca. 1.58 Å) within the normal range found for similar Ga(III) complexes.[33, 34] UV-Vis spectrophotometric absorption analysis confirmed that the ligand and complexes were stable within 48 h in 0.1% DMSO aqueous solution (Fig. S1).

Electrochemistry.

As our recent studies have shown, intracellular ROS levels are significantly elevated when NCI−H460 cells are exposed to

View Article Online
DOI: 10.1039/C8NJ00697K

gallium complexes. Therefore, investigating the electrochemistry of Ga(III) complexes is important. Cyclic voltammetry results indicate that the Ga(III) complex does not exert any redox activity (Fig.2). A facile, reversible, single electron redox process was observed when ferric(III) nitrate was added to the Ga(III) complex solution, which indicates that

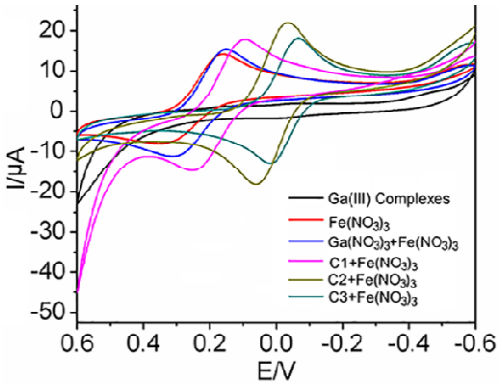

Fig 2. Cyclic voltammograms of Ga(III) complexes, $Fe(NO_3)_3$, $Ga(NO_3)_3$ + $Fe(NO_3)_3$, C1 + $Fe(NO_3)_3$, C2 + $Fe(NO_3)_3$ and C3 + $Fe(NO_3)_3$.

iron substitutes gallium to form Fe(III)–thiosemicarbazone complexes. The cathodic shift in the $Fe^{III/II}$ redox potentials reveals that oxidation–reduction reactions are prone to occur (Fig.2).

Anticancer properties of Ga complexes.

The anticancer activity of the 2-benzoylpyridine thiosemicarbazone (BpT) series against SK-N-MC neuroepithelioma cells and human DMS-53 lung carcinoma cells has been well characterized.[34-37] Similar results were obtained in our study using the NCI-H460 human lung cancer cells, BEL-7402 human hepatoma cells and T24 human bladder cancer cells (Table 1), which confirms the extensive antiproliferative activity of BpT ligands. IC_{50} (the half-maximal inhibitory concentration), which refers to the concentration of an inhibitor that is required for 50% inhibition of cell growth, was determined by MTT assay. These Ga(III) complexes were compared with corresponding ligands and a relevant positive control (3-AP). The ligands and gallium complexes exhibited a lower toxicity to human fetal lung fibroblast (MRC-5) cells than that of cancer cells (Table 1).

Table 1 IC_{50} (μM) values of ligands and Ga(III) complexes toward the cell lines for 48h.

	IC_{50} (μM)			
	NCI−H460	BEL-7402	T24	MRC-5
3−AP	4.23 ± 0.52	5.01 ± 0.43	4.18 ± 0.35	-
L1	17.54 ± 2.2	15.54 ± 0.98	19.06 ± 1.99	67.34 ± 4.64
L2	6.88 ± 1.3	8.88 ± 0.56	9.32 ± 1.01	32.43 ± 2.06
L3	1.08 ± 0.23	2.69 ± 0.37	1.23 ± 0.22	21.87 ± 1.28
C1	4.89 ± 0.34	4.53 ± 0.54	4.98 ± 0.29	43.55 ± 2.39
C2	2.65 ± 0.22	3.27 ± 0.28	3.52 ± 0.19	24.28 ± 2.03
C3	0.25 ± 0.09	0.54 ± 0.07	0.37 ± 0.03	18.37 ± 1.58
$Ga(NO_3)_3$	> 100	> 100	> 100	> 100

These ligands and complexes showed a good activity against these cancer cell lines, whereas $Ga(NO_3)_3$ (100 μM) alone presented no pronounced antiproliferative effect (Table 1). The antitumor activity of L3 (IC_{50} = 1.08 ± 0.23 μM) was significantly ($p < 0.05$) higher than those of L1 (IC_{50} = 17.54 ± 2.2 μM), L2 (IC_{50} = 6.88 ± 1.3 μM), and 3−AP (IC_{50} = 4.23 ± 0.52 μM) after a 48 h incubation with NCI−H460. Interestingly the anticancer activities of C1, C2, and C3 in the MTT assay were better than those of their corresponding ligands. In terms of IC_{50} values, C3 (IC_{50} = 0.25 ± 0.09 μM) was the most effective among the Ga(III) complexes (compared with C1 with IC_{50} = 4.89 ± 0.34 μM and C2 with IC_{50} = 2.65± 0.22 μM) for NCI−H460 cells. This trend can be explained by the lipophilic group (phenyl, and dimethyl) of the N4 substituents.[34] Notably, the increased activity was more strongly connected to the different metal binding ability of the dimethylated compounds compared to the unsubstituted ones.[38,39] The increased anticancer activity of the Ga(III) complexes relative to that of the ligand was observed probably because the dissociation of the complexes releases two ligands, possibly in pH 7.4 solution.

Potential anticancer mechanism of Ga(III) complexes.

Richardson et al. have demonstrated that the mechanism of action of BpT series involves the Fe chelation and redox cycling of its Fe complex to ROS, hydroxyl radicals (OH•): this occurrence leads to the damage of essential biomolecules within cells.[35, 40] However, the antitumor mechanism of thiosemicarbazide Ga(III) complex has not been systematically studied. As the gallium complexes significantly promote NCI-H460 cell apoptosis, studying their antitumor mechanisms is important. We investigated intracellular Ca^{2+} and intracellular ROS, the mitochondrial membrane potential, and the expression of mitochondrial pathway-related proteins to explore the pathways by which gallium complexes promote NCI-H460 cell apoptosis.

Ga(III) complexes induce intracellular Ca^{2+} release.

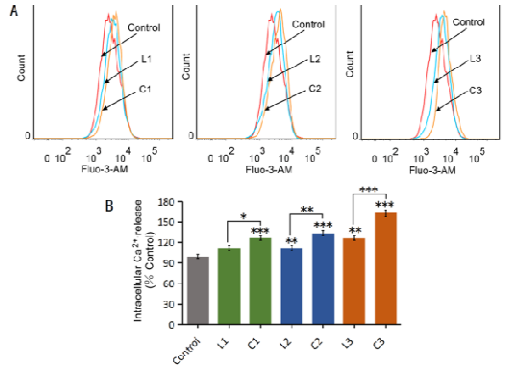

Fig. 3. Thiosemicarbazone ligands (L1-L3) and Ga(III) complexes (C1-C3) induced intracellular release of Ca2+ in cancer cells. (A) Intracellular Ca2+ was detected in NCI−H460 cells by flow cytometry; (B) quantification of the flow cytometric results in (A). Results are the mean ± SD (n = 6−7): *p < 0.05, **p < 0.01, ***p < 0.001.

View Article Online
DOI: 10.1039/C8NJ00697K

Metal-based antitumor drugs induce Ca^{2+} signaling by the intracellular release of the Ca^{2+} ion pool.[8] Intracellular Ca^{2+} release was assayed in Ga(III) complex-treated NCI-H460 cells by flow cytometry. After 30 min incubation, thiosemicarbazone ligands (except L1) and Ga(III) complexes significantly ($p < 0.01$) increased release of intracellular Ca^{2+} (Fig. 3). Interestingly, Ga(III) complexes initiated intracellular Ca^{2+} release significantly ($p < 0.05$) higher than the ligand.

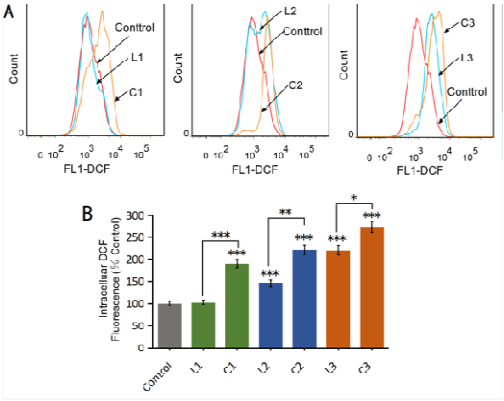

Fig. 4. Thiosemicarbazone ligands (L1-L3) and Ga(III) complexes (C1-C3) increased the intracellular ROS levels in cancer cells. (A) Intracellular ROS was detected in NCI−H460 cells; (B) quantification of the flow cytometric results in (A). Results are the mean ± SD (n = 6−7): *p < 0.05, **p < 0.01, ***p < 0.001.

Intracellular calcium levels were 126%, 133% and 162% relative to the control after C1, C2 and C3-treatment, respectively.

Ga(III) complexes increased the intracellular ROS levels.

The release of intracellular Ca^{2+} induced the production of ROS in cancer cells.[41] Fluorescent DCF probe and flow cytometry were employed to evaluate the ability of Ga(III) complexes to affect the level of intracellular ROS in NCI-H460 cells (Fig. 4). The DCF fluorescence peaks of the cells treated with Ga(III) complexes were shifted to the right relative to those of the control cells, indicating that these complexes increased the intracellular ROS levels. Ga(III) complexes significantly ($p < 0.001$) the increased intracellular ROS levels relative to the ligands and control (Fig. 4). The quantification of the DCF fluorescence peaks in part A of Fig. 4 proved that C3 caused a significant ($p < 0.001$) increase in H_2DCF oxidation to 273% ± 10% of that of the control cells. Furthermore, C3 was found to be 51% and 83% more effective than C2 and C1, respectively, in inducing intracellular ROS.

Mitochondrial membrane potential assay.

The change in intracellular ROS level is an important factor affecting the mitochondrial membrane potential.[42] The change in the mitochondrial transmembrane potential was detected by JC-1 (a kind of lipophilic fluorescent probe). After staining by JC-1, the color of the mitochondrial membrane changed from red to green when the membrane potential decreased and assayed by flow cytometry (Fig. 5). The mitochondrial transmembrane of the NCI-H460 cells treated with Ga(III) complexes presented a green fluorescence signal, whereas the vehicle-treated controls showed a red signal, which meant that Ga(III) complexes, especially C3, can lead to the collapse of the mitochondrial transmembrane potential (Δψm).

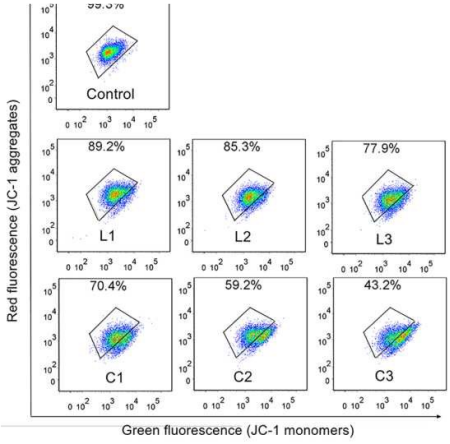

Fig. 5. Assay of NCI−H460 cells mitochondrial membrane potential with JC−1 as fluorescence probe staining method.

Ga(III) complexes regulate the expression of mitochondrial pathway-related proteins.

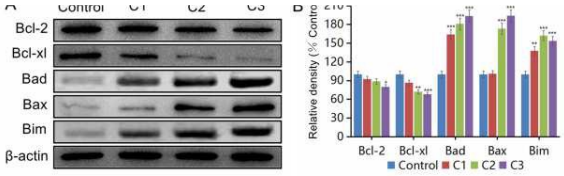

Fig. 6. (A) Western blot analysis of Bcl−2, Bcl−xl, Bax, Bad and Bim levels after Ga(III) complexes treatment. β−actin was used as internal control. (B) Densitometric analysis of the expression of Bcl−2, Bcl−xl, Bax, Bad and Bim. The percentage values are those relative to the control. Results are the mean ± SD (n = 6−7): *p < 0.05, **p < 0.01, ***p < 0.001.

The Bcl−2 family proteins play a critical role in the intrinsic mitochondrial signal pathway of cell apoptosis.[42-45] The influence of Ga(III) complexes on the expression levels of these proteins in NCI−H460 cells were analyzed by Western blot. After incubation with C1, C2 and C3, the expression levels of antiapoptotic proteins (Bcl−2 and Bcl−xl) gradually decreased, whereas those of proapoptotic proteins (Bax, Bim and Bad) gradually increased (Fig. 6). The ratio of Bax/Bcl−2 increased from 1.00-fold to 1.09, 1.97, and 2.44-folds after incubation with C1, C2 and C3, respectively (Fig. 6). The increase in Bax/Bcl−2 ratio leads to the enhanced mitochondrial membrane permeability, which is favorable for the release of apoptogenic factors.

The consumption of mitochondrial transmembrane potential (Δψm) promotes the release of apoptosis factors and causes the

View Article Online
DOI: 10.1039/C8NJ00697K

irreversible cell apoptosis.[46] The release of cytochrome C (Cyt C) and the activation of caspase family proteins (caspase 3 and 9) play a key role in the mitochondria mediated apoptosis pathway.[47, 48] To determine the role of the promotion of cell apoptosis factors during Ga(III) complex−induced apoptosis in NCI−H460 cells, we examined the protein levels of Cyt C, activated caspase 3 and 9, and their enzymatic activities (Fig. 7). Incubating NCI-H460 cells with C1, C2 and C3 raised the levels of Cyt C by 1.20, 1.38 and 1.51-folds relative to that of control, respectively. After incubation with C1, C2, and C3, the activated caspase 3 protein levels increased by 1.04, 1.12, and 1.18-folds, respectively, and the activated caspase 9 protein levels by 1.08, 1.28, and 1.48-folds, respectively, relative to that of the control, respectively (Fig. 7). The release of Cyt C leads to the activation of downstream caspase family proteins and affects the corresponding substrates; ultimately, cell apoptosis ensues. [47]

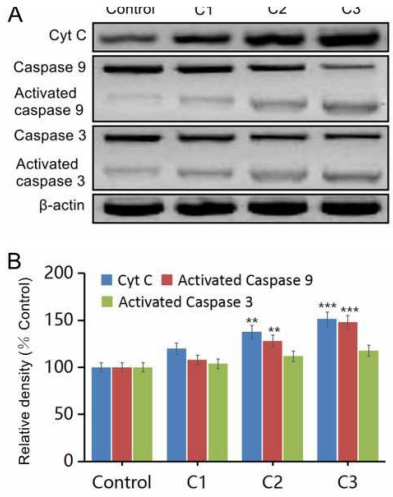

Fig. 7. (A) Western blot analysis of Cyt C, Caspase 9 and 3 levels after Ga(III) complexes treatment. β−actin was used as internal control. (B) Densitometric analysis of the expression of Cyt C, Caspase 9 and 3. The percentage values are those relative to the control. Results are the mean ± SD (n = 6−7): *p < 0.05, **p < 0.01, ***p < 0.001.

Ga(III) complexes promote cell apoptosis.

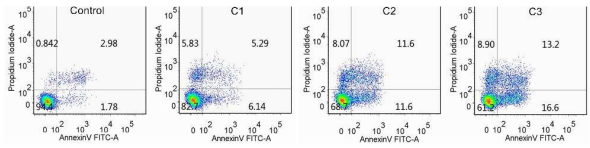

Fig. 8. The apoptosis analysis of the NCI−H460 cells treated by Ga(III) complexes (5 μM) for 12 h, and representative dot plots of PI and annexin V double staining. (A) Control; (B−D) C1−C3.

MTT experiments demonstrated that the coordination of ligands with Ga(III) ions can cause marked increases in anticancer activity. Therefore, the antitumor activity of the three Ga(III) complexes has aroused our interest. NCI−H460 cells treated with Ga(III) complexes (5 μM) for 12 h showed increased apoptosis relative to that of the vehicle-treated controls under Annexin V−FITC/PI staining (Fig. 8). The percentages of the cells where C1−C3 promoted early apoptosis were 4.36%, 9.82% and 14.82%, respectively, relative to the control. Results revealed that C3 was found to be 5% and 10% more effective than C2 and C1, respectively, in inducing cell early cell apoptosis (Fig. 8). Our results illustrated that the intrinsic mitochondrial signal pathway is involved in Ga(III) complex-induced apoptosis.

Experimental

Materials.

2−Benzoylpyridine, 4−Phenyl−3−thiosemicarbazide, 4,4−Dimethyl−3−thiosemicarbazide, N−Aminothiourea, $Ga(NO_3)_3$ and solvents were purchased from Energy Chemical Company (Shanghai) without further purification. Ultrapure water was used in all experiments. Elemental analyses (C, N, and H) were carried out on a PerkineElmer 2400 analyzer. Primary (Anti-Bcl-2 antibody, Anti-Bcl−xl antibody, Anti-Bax antibody, Anti-Bad antibody, Anti-Bim antibody, Anti-Cyt C antibody, Anti-Caspase 9 antibody, Anti-Caspase 3 and Anti-β-Actin antibody) and secondary antibodies (Goat Anti-Rabbit IgG H&L) were purchased from Abcam Company (Shanghai, China). The NCI_H460, BEL-7402, T24 and MRC-5 cell lines were purchased from Chinese Academy of Sciences (Shanghai, China).

Synthesis and characterization of Ga(III) complexes.

The ligands L1−L3 were all prepared by the published methods.[26, 51, 52] Briefly, 10 mL of 2−Benzoylpyridine (10 mmol) MeOH solution was added drop wise into 10 mL of thiosemicarbazide or its derivatives (10 mmol) water solution with stirring. The mixture was added with 0.05 mL of glacial acetic acid and refluxed for 4 h. When the solution was cooled, the thiosemicarbazone precipitate was filtered, washed with EtOH (5 mL) and diethyl ether (5 mL), and then dried in a vacuum desiccator.

2−Benzoylpyridine thiosemicarbazone (L1): yield 81%. *Anal. Calcd* for $C_{13}H_{12}N_4S$: C, 60.92; H, 4.72; N, 21.86; S, 12.51. Found: C, 60.90; H, 4.71; N, 21.87; S, 12.53. ^{1}H NMR (400 MHz, D_2O : DMSO-d_6 = 7 : 3, pH =7.5): δ 12.43 (s, 1H), δ 9.46 (s, 1H), 9.02 (s, 1H), 8.92-8.88 (s, 1H), 8.83 (s, 2H), 8.62 (s, 1H), 8.35 (s, 1H), 8.20 (s, 1H), 8.08 (td, J=7.8, 1.5Hz, 1H), 7.87 (s, 2H). MS m/z (%) 255.07 (M − H, 100).

2−Benzoylpyridine 4−phenyl−3−thiosemicarbazone (L2): yield 79%. *Anal. Calcd* for $C_{19}H_{16}N_4S$: C, 68.65; H, 4.85; N, 16.85; S, 9.64. Found: C, 68.61; H, 4.87; N, 16.83; S, 9.68. ^{1}H NMR (400 MHz, D_2O : DMSO-d_6 = 7 : 3, pH =7.5): δ 13.15 (s, 1H), 10.34 (s, 1H), 8.89 (d, J = 4.2 Hz, 1H), 8.05 (td, J = 7.9, 1.8 Hz, 1H), 7.73 (dt, J = 8.6, 3.9 Hz, 2H), 7.61 – 7.55 (m, 3H), 7.53 – 7.45 (m, 3H), 7.40 (dd, J = 4.3, 3.2 Hz, 3H), 7.25 (dd, J = 7.3, 4.3 Hz, 1H). MS m/z (%) 321.10 (M − H, 100).

2−Benzoylpyridine 4,4−dimethyl−3−thiosemicarbazone (L3): yield 67%. *Anal. Calcd* for $C_{15}H_{16}N_4S$: C, 63.35; H, 5.67; N, 19.70; S, 11.27. Found: C, 63.40; H, 5.64; N, 19.72; S, 11.23.

View Article Online
DOI: 10.1039/C8NJ00697K

^{1}H NMR (400 MHz, D_2O : DMSO-d_6 = 7 : 3, pH =7.5): δ 12.59 (s, 1H), δ 8.93-8.84 (m, 2H), 8.45 (dd, J=12.0, 4.3 Hz, 1H), 8.02 (d, J=1.7 Hz, 2H), 7.69-7.67 (m, 2H), 7.58 (d, J = 7.5Hz, 1H), 3.37 (s, 6H). MS m/z (%) 283.10 (M − H, 100).

The synthesis method of complexes C1−C3 is as follows. A solution of $Ga(NO_3)_3$ (0.5 mmol) in MeOH (10 mL) was added drop wise into 10 mL of the relevant ligands (1 mmol) MeOH solution with stirring, and refluxed for 30 min. The solution was slowly volatilized at room temperature, and the yellow crystals formed after a few days. The crystals were filtered, washed with EtOH (5 mL) and diethyl ether (5 mL) and dried in a vacuum desiccator.

2−Benzoylpyridine thiosemicarbazone Ga(III) (C1): yield 67%. *Anal. Calcd* for $C_{26}H_{22}GaN_9O_3S_2$: C, 48.62; H, 3.45; N, 19.62; O, 7.47; S, 9.98. Found: C, 48.66; H, 3.43; N, 19.63; O, 7.45; S, 9.96. MS m/z (%) 578.07 (M − H, 100). ^{1}H NMR (400 MHz, D_2O : DMSO-d_6 = 7 : 3, pH =7.5): δ 9.90 (d, J = 6.8 Hz, 2H), δ 9.70 (s, 4H), 8.81-8.87 (m, 2H), 8.55 (td, J = 7.2, 1.3 Hz, 1H), 8.32 (dd, J = 8.6, 0.7 Hz,2H), 7.71-7.68 (m, 4H), 7.66 (s, 4H), 7.45 (dd, J=10, 7.2Hz, 2H).

2−Benzoylpyridine 4−phenyl−3−thiosemicarbazone Ga(III) (C2): yield 71%. *Anal. Calcd* for $C_{38}H_{30}GaN_9O_3S_2$: C, 57.44; H, 3.81; N, 15.87; O, 6.04; S, 8.07. Found: C, 57.46; H, 3.78; N, 15.84; O, 6.08; S, 8.05. MS m/z (%) 730.12 (M − H, 100). ^{1}H NMR (400 MHz, D_2O : DMSO-d_6 = 7 : 3, pH =7.5): δ 10.44 (s, 2H), 8.34 (d, *J* = 5.0 Hz, 2H), 8.25 (d, *J* = 1.2 Hz, 2H), 7.91 (d, *J* = 6.5 Hz, 4H), 7.81 – 7.71 (m, 10H), 7.53 (d, *J* = 8.0 Hz, 4H), 7.17 (t, *J* = 7.8 Hz, 4H), 7.02 (s, 2H).

2−Benzoylpyridine 4,4−dimethyl−3−thiosemicarbazone Ga(III) (C3): yield 83%. *Anal. Calcd* for $C_{30}H_{30}GaN_9O_3S_2$: C, 51.59; H, 4.33; N, 18.05; O, 6.87; S, 9.18. Found: C, 51.54; H, 4.36; N, 18.02; O, 6.89; S, 9.22. MS m/z (%) 634.13 (M − H, 100). ^{1}H NMR (400 MHz, D_2O : DMSO-d_6 = 7 : 3, pH =7.5): δ 8.17 (s, 4H), 7.89 – 7.82 (m, 4H), 7.69 (dd, *J* = 11.7, 4.1 Hz, 8H), 7.64 (s, 2H), 3.18 (d, *J* = 7.3 Hz, 6H), 3.09 (s, 6H).

Determination of structure of Ga(III) complexes.

X−ray diffraction data of Ga(III) complexes were collected by a Bruker SMART Apex II CCD diffract meter using graphite−monochromatic Mo−Kα (λ = 0.71073 Å) radiation at 296.15 K, and then adsorption corrections with SADABS. The structures were solved and refined against F2 by full−matrix least−squares methods using the Olex2 software. [53] C, N, Ga and O atoms were refined anisotropic ally. H atoms were added in theoretically ideal positions by Olex2. The Crystal Data of three Ga(III) complexes are showed in Table 1. Selected bond lengths (Å) and angles (deg) are showed in Table S1. The crystal structure analysis data can get from Cambridge Crystallographic Data Centre via http://www.ccdc.cam.ac.uk/data_request/cif.

Cyclic voltammetry.

Cyclic voltammetry was performed using a CHI660E electrochemical workstation (Shanghai Chenhua Instruments, China). Glassy carbon, aqueous Ag/AgCl and Pt wire were used for working, reference and auxiliary electrode, respectively. All complexes were at 1 mM concentration in DMSO/H_2O (70:30 v/v). The supporting electrolyte was Bu_4NClO_4 (0.1 M), and the solutions were purged with nitrogen prior to measurement. The sweep rate was 100 mVs^{-1}.

Cytotoxicity assay in vitro.

The ligands and Ga(III) complexes were dissolved in DMSO as 10mM mother solutions and diluted in cell culture medium to needed concentration. NCI−H460 cell line was cultivated at 37 □ in a humidified atmosphere of 5% CO_2/95% air in an incubator. Cell toxicity test is determined by 3-(4,5-dimethyl-2-thiazolyl)-2,5-diphenyl-2-H-tetrazolium bromide solution (MTT) assay and performed according to the published methods. Briefly, 180 μL of 5×10^4 cells per well were seeded in 96 well plates and cultivated for 24 h in a humidified atmosphere of 5% CO_2/95% air in an incubator. Then the compounds at various concentrations were added into per well and incubated for 48 h. At the end of the experimental, every well was added with 10 μL MTT and incubated for 4 h at 37 □. After removing the supernatant, 100 μL of DMSO were added. The absorbance with 570/630 nm double wavelength measurement of per well were read by enzyme labelling instrument. IC_{50} values were calculated by the nonlinear multipurpose curve−fitting program Graph Pad Prism. All of the tests were repeated in least three measurements.

Intracellular Ca^{2+} mobilization assay.

Ca^{2+} was measured by flow cytometry according to the specification of the Fluo-3 AM (calcium fluorescence probe) assay kit (Beyotime, Suzhou) based on the fluorescence method. 5 mL of 5×10^5 cells/mL NCI−H460 cells were seeded in 7.5 cm plates and cultivated at least 12 h before treatment. Cells were incubated with 25 μM of L1-L3 and C1−C3 in cell culture medium for 30 min at 37 □. After washed twice with PBS, the samples were incubated with 5 μM Fluo-3 AM for 30 min at 37 □. Followed by three washes with PBS. Cells were suspended in Ca^{2+}-free PBS (0.5 mL) and Fluo-3 fluorescence intensity was analysed by flow cytometry.

Intracellular ROS measurements.

Intracellular ROS generation was measured by Flow Cytometer according to the specification of the Reactive oxygen species assay kit (Beyotime, Suzhou). NCI−H460 cells were incubated with 25 μM of L1-L3 and C1−C3 in serum−free cell culture medium for 30 min at 37 □. The cells were incubated with 2 μM H_2DCF−DA for 30 min at 37 ℃. After washed twice with serum free medium, the samples were assayed by Flow Cytometer with excitation wavelength at 488 nm and emission wavelength at 525 nm. Data were analysed by FlowJo software.

The change of mitochondrial membrane potential assay.

Intracellular change of mitochondrial membrane potential was observed by fluorescent inverted microscope according to the specification of the JC−I assay kit (Beyotime, Suzhou). 2mL of 1×10^5 cells/mL were seeded in 6 well plates and cultivated for 24 h before treatment, and then incubated with the L1-L3 and C1−C3 (5 μM) for 30 min at 5% CO_2 and 37 ℃. The cells were incubated with 1 μM 1 μg/mL of 5, 5, 6, 6′−tetrachloro−1, 1', 3, 3′−tetraethyl−imidacarbocyanineiodide iodide (JC−1) for 30 min at 37 ℃. After washed twice with cell culture media, the

View Article Online
DOI: 10.1039/C8NJ00697K

cells were detected by flow cytometry. Data were analysed by FlowJo software.

Western blot analysis.

5 mL of 5×10^5 cells/mL NCI−H460 cells were seeded in 10 cm plates and cultivated at least 12 h before treatment. Cells were incubated with 5 μM of C1−C3 in cell culture medium for 12 h at 37 □ in a humidified atmosphere of 5% CO_2/95% air in an incubator. NCI−H460 cells were cracked in lysis buffer. Insoluble substance was separated by centrifuge for 30 min at 10,000g. Protein concentration was determined by the BCA assay kit (Beyotime, Suzhou). SDS–polyacrylamide gel electrophoresis was done by loading equal amounts of sample total proteins in each canal. Proteins were then metastasized to vinylidene difluoride membranes (Millipore) and blocked with 5% defatted milk in TBST buffer for 1 h. The membranes were incubated with 1:1000 dilutions in 5% defatted milk of primary antibodies for 12h at 4 □. After being washed for two or three times with TBST for 30 min, the membranes were incubated with secondary antibodies at 1:1000 dilutions for 1 h at 25 □ and then washed for two or three times with TBST. The immunoreactivity was visualized by Amersham ECL Plus (Amersham) western blotting detection. The β−actin was used for detect amount of proteins of each lane. Quantitative analysis of electrophoretic results was performed by Image-Pro software. The gray value of the target protein is equal to the ratio of its IOD to the β−actin's IOD value.

Cell apoptosis assay.

The apoptotic events induced by the Ga(III) complexes (C1−C3) were assayed by Flow Cytometer (BD, Shanghai) according to the specification for the Annexin V−FITC Apoptosis Detection Kit (BD, Shanghai). In this experiment, 2mL of 1×10^5 cells/mL were seeded in 6 well plates and cultivated for 24 h, which were incubated with the C1−C3 (5 μM) for 12 h at 5% CO_2 and 37 □. The NCI−H460 cells were suspended in 200 μL binding buffer, then 5μL of Annexin V and PI were added to each sample. After 15 min incubation at 25 □, the samples were assayed by Flow Cytometer. Cell apoptosis rate were analysed by FlowJo software.

Statistical analysis.

All of the tests were repeated in least three measurements. Student's t test was applied to evaluate the significant difference. Results were represented as mean ± standard deviation (SD). It was significant when $P < 0.05$.

Conclusions

Our results revealed that the anticancer activity of these three Ga(III) compounds are significantly higher than those of their corresponding ligands. Modifying at the N4 position of the ligand with lipotropic groups can also increase antitumor activity of the Ga (III) complexes. The anticancer mechanism of Ga (III) complexes may involve Ca^{2+} signaling triggers and the intrinsic ROS−mediated mitochondrial single pathway, which company the regulation of Bcl-family proteins and the activation of caspase family proteins.

Redox-inactive Ga(III) complexes cannot produce ROS.[32] However, substantial evidence has indicated that intracellular ROS levels are significantly raised after gallium complex treatment.[8, 49, 50] Electrochemical studies have shown that Ga(III) complexes do not possess redox properties, whereas Fe(III) complexes exhibit good redox activity. Because the stability constant of the Fe(III)-thiosemicarbazone complexes is higher than that of the gallium(III) complexes, we speculated that some gallium ions of the complexes were replaced by intracellular iron ions to produce ROS. Ga(III) complexes initiated the release of intracellular Ca^{2+}, which led to the increase in ROS levels and collapse of mitochondrial membrane potential. In conclusion, the Ga (III) complexes promoted apoptosis as a result of a combination of multiple apoptotic pathways such as Ca^{2+} signaling triggers and ROS-mediated mitochondrial pathways. These results may contribute to the development of novel Ga(III) anticancer agents.

Conflicts of interest

There are no conflicts to declare.

Acknowledgements

This work was supported by National Nature Science Foundations of China (81571812), Priority Academic Program Development of Jiangsu Higher Education Institutions (1107047002), the Fundamental Research Funds for the Central Universities and Postgraduate Research& Practice Innovation Program of Jiangsu Province (KYCX17_0135). The research was also supported by the Scientific Research Foundation of Graduated School of Southeast University (YBJJ1787).

Notes and references

‡ CCDC 1488960-1488962 contain the supplementary crystallographic data for this paper. Selected Bond Lengths (Å) and Angles (deg). The UV-Visible absorption of ligands and Ga complexes.

1 P. Collery, B. Keppler, C. Madoulet, B. Desoize, *Critical reviews in oncology/hematology*, 2002, **42**, 283.
2 V. Nikolova, S. Angelova, N. Markova, T. Dudev, *The Journal of Physical Chemistry B* 2016, **120**, 2241.
3 M. A. Jakupec, B. K. Keppler, *Current Topics in Medicinal Chemistry*, 2004, **4**, 1575.
4 J. A. Lessa, M. A. Soares, R. G. Dos Santos, I. C. Mendes, L. B. Salum, H. N. Daghestani, A. D. Andricopulo, B. W. Day, A. Vogt, HBeraldo, *BioMetals* 2013, **26**, 151.
5 T.S. Lobana, R. Sharma, G. Bawa, S. Khanna, Coord. Chem. Rev., 2009, **253**, 977.
6 T.S. Lobana, RSC Adv., 2015, **5**, 37231.
7 C. R. Chitambar, W. E. Antholine, *Antioxidants & Redox Signaling,* 2013, **18**, 956.
8 R. Gogna, E. Madan, B. Keppler, U. Pati, *British Journal of Pharmacology,* 2012, **166**, 617.
9 L. R. Bernstein, T. Tanner, C. Godfrey, B. Noll, *Metal-based drugs,* 2000, **7**, 33.
10 C. R. Kowol, R. Trondl, P. Heffeter, V. B. Arion, M. A. Jakupec, A. Roller, M. Galanski, W. Berger, B. K. Keppler, *Journal of medicinal chemistry,* 2009, **52**, 5032.

View Article Online
DOI: 10.1039/C8NJ00697K

11 C. R. Chitambar, J. P. Wereley, S. Matsuyama, *Molecular cancer therapeutics,* 2006, **5**, 2834.
12 C. R. Chitambar, D. P. Purpi, *Leukemia researchs,* 2010, **34**, 950.
13 Y. Hata, A. Sandler, P. J. Loehrer, G. J. Sledge, G. Weber, *Oncology Research,* 1994, **6**, 19.
14 E. A. Akam, E. Tomat, *Bioconjug Chem.,* 2016, **27**, 1807.
15 Y. Yu, D. S. Kalinowski, Z. Kovacevic, A. R. Siafakas, P. J. Jansson, C. Stefani, D. B. Lovejoy, P. C. Sharpe, P. V. Bernhardt, D. R. Richardson, *Journal of Medicinal Chemistry*, 2009, **52**, 5271.
16 R. A. Finch, M. Liu, S. P. Grill, W. C. Rose, R. Loomis, K. M. Vasquez, Y. Cheng, A. C. Sartorelli, *Biochem Pharmacol,* 2000, **59**, 983.
17 D. S. Kalinowski, P. C. Sharpe, P. V. Bernhardt, D. R. Richardson, *Journal of Medicinal Chemistry*, 2007, **50**, 6212.
18 B. M. Zeglis, V. Divilov, J. S. Lewis, *Journal of Medicinal Chemistry*, 2011, **54**, 2391.
19 A. E. Stacy, D. Palanimuthu, P. V. Bernhardt, D. S. Kalinowski, P. J. Jansson, D. R. Richardson, *Journal of medicinal chemistry,* 2016, **59**, 8601.
20 A. Dobrova, S. Platzer, F. Bacher, M. N. Milunovic, A. Dobrov, G. Spengler, E. A. Enyedy, G. Novitchi, V. B. Arion, *Dalton Transactions,* 2016, **45**, 13427.
21 S. Hosseinpour, S.A. Hosseini-Yazdi, J. White, W.S. Kassel, N. A. Piro, *Polyhedron*, 2017, **121**, 236.
22 D. R. Richardson, D. S. Kalinowski, V. Richardson, P. C. Sharpe, D. B. Lovejoy, M. Islam, P. V. Bernhardt, *Journal of Medicinal Chemistry,* 2009, **52**, 1459.
23 C. Santini, M. Pellei, V. Gandin, M. Porchia, F. Tisato, C. Marzano, *Chemical Reviews,* 2014, **114**, 815.
24 Y. Gou, J. Wang, S. Chen, Z. Zhang, Y. Zhang, W. Zhang, F. Yang, *European Journal of Medicinal Chemistry,* 2016, **123**, 354.
25 É. A. Enyedy, N. V. Nagy, É. Zsigó, C. R. Kowol, V. B. Arion, B. K. Keppler, T. Kiss, *European Journal of Inorganic Chemistry*, 2010, **11**, 1717.
26 J. Qi, Y. Gou, Y. Zhang, K. Yang, S. Chen, L. Liu, X. Wu, T. Wang, W. Zhang, F. Yang, *Journal of Medicinal Chemistry,* 2016, **59**, 7497.
27 J. Qi, J. Deng, K. Qian, L. Tian, J. Li, K. He, X. Huang, Z. Cheng, Y. Zheng, Y. Wang, *European Journal of Medicinal Chemistry,* 2017, **134**, 34.
28 P. V. Bernhardt, P. C. Sharpe, M. Islam, D. B. Lovejoy, D. S. Kalinowski, D. R. Richardson, *Journal of Medicinal Chemistry,* 2009, **52**, 407.
29 C. R. Kowol, R. Berger, R. Eichinger, A. Roller, M. A. Jakupec, P. P. Schmidt, V. B. Arion, B. K. Keppler, *Journal of Medicinal Chemistry,* 2007, **50**, 1254.
30 L. A. Torre, F. Bray, R. L. Siegel, J. Ferlay, J. Lortet-Tieulent, A. Jemal, *CA: a cancer journal for clinicians*, 2015, 65, 87.
31 J. G. Da Silva, L. S. Azzolini, S. M. S. V. Wardell, J. L. Wardell, H. Beraldo, *Polyhedron,* 2009, **28**, 2301.
32 C. R. Kowol, R. Trondl, P. Heffeter, V. B. Arion, M. A. Jakupec, A. Roller, M. Galanski, W. Berger, B. K. Keppler, *Journal of Medicinal Chemistry,* 2009, **52**, 5032.
33 J. Qi, Y. Zheng, K. Qian, L. Tian, G.X. Zhang, Z. Cheng, Y. Wang, *Journal of inorganic biochemistry*, 2017, **177**, 110.
34 C. Stefani, P. J. Jansson, E. Gutierrez, P. V. Bernhardt, D. R. Richardson, D. S. Kalinowski, *Journal of Medicinal Chemistry,* 2013, **56**, 357.
35 C. Stefani, G. Punnia-Moorthy, D. B. Lovejoy, P. J. Jansson, D. S. Kalinowski, P. C. Sharpe, P. V. Bernhardt, D. R. Richardson, *Journal of Medicinal Chemistry,* 2011, **54**, 6936.
36 Y. Yu, Y. S. Rahmanto, D. R. Richardson, *British Journal of Pharmacology,* 2012, **165**, 148.
37 Z. L. Guo, D. R. Richardson, D. S. Kalinowski, Z. Kovacevic, K. C. Tan-Un, G. C. Chan, *Journal of hematology & oncology,* 2016, **9**, 98.
38 C. R. Kowol, W. Miklos, S. Pfaff, S. Hager, S. Kallus, K. Pelivan, M. Kubanik, E. A. Enyedy, W. Berger, P. Heffeter and B. K. Keppler, *J MED CHEM*, 2016, **59**, 6739-6752.
39 P. Heffeter, C. Pirker, C. R. Kowol, G. Herrman, R. Dornetshuber, W. Miklos, U. Jungwirth, G. Koellensperger, B. K. Keppler and W. Berger, *BIOCHEM PHARMACOL*, 2012, **83**, 1623.
40 P. J. Jansson, P. C. Sharpe, P. V. Bernhardt, D. R. Richardson, *Journal of Medicinal Chemistry,* 2010, **53**, 5759.
41 Y. O. Son, J. C. Lee, J. A. Hitron, J. Pan, Z. Zhang, X. Shi, *Toxicological Sciences,* 2010, **113**, 127.
42 H. J. Lee, Y. K. Oh, M. Rhee, J. Y. Lim, J. Y. Hwang, Y. S. Park, Y. Kwon, K. H. Choi, I. Jo, S. I. Park, B. Gao, W. H. Kim, *Journal of molecular biology,* 2007, **369**, 967.
43 T. Yoshino, H. Shiina, S. Urakami, N. Kikuno, T. Yoneda, K. Shigeno, M. Igawa, *Clinical Cancer Research,* 2006, **12**, 6116.
44 G. Tang, Z. Nikolovska-Coleska, S. Qiu, Yang, Y. C. J. Guo, S. Wang, *Journal of medicinal chemistry,* 2008, **51**, 717.
45 V. P. Androutsopoulos, K. C. Ruparelia, A. Papakyriakou, H. Filippakis, A. M. Tsatsakis, D. A. Spandidos, *European Journal of Medicinal Chemistry,* 2011, **46**, 2586.
46 E. H. Cheng, M. C. Wei, S. Weiler, R. A. Flavell, T. W. Mak, T. Lindsten, S. J. Korsmeyer, *Molecular cell,* 2001, **8**, 705.
47 C. N. Kim, X. Wang, Y. Huang, A. M. Ibrado, L. Liu, G. Fang, K. Bhalla, *Cancer Res,* 1997, **57**, 3115.
48 Y. Y. Li, Z. Zhang, Z. H. Wang, H. W. Wang, L. Zhang, L. Zhu, *Toxicol Lett,* 2009, **189**, 166.
49 C. R. Chitambar, D. P. Purpi, J. Woodliff, M. Yang, J. P. Wereley, *J Pharmacol Exp Ther,* 2007, **322**, 1228.
50 M. Yang, C. R. Chitambar, *Free Radic Biol Med,* 2008, **45**, 763.
51 J. Qi, S. Liang, Y. Gou, Z. Zhang, Z. Zhou, F. Yang, H. Liang, *European Journal of Medicinal Chemistry,* 2015, **96**, 360.
52 D. S. Kalinowski, Y. Yu, P. C. Sharpe, M. Islam, Y. T. Liao, D. B. Lovejoy, N. Kumar, P. V. Bernhardt, D. R. Richardson, *Journal of medicinal chemistry,* 2007, **50**, 3716.
53 O. V. Dolomanov, L. J. Bourhis, R. J. Gildea, J. A. K. Howard, H. Puschmann, *Journal of Applied Crystallography,* 2009, 42, 339.

View Article Online
DOI: 10.1039/C8NJ00697K

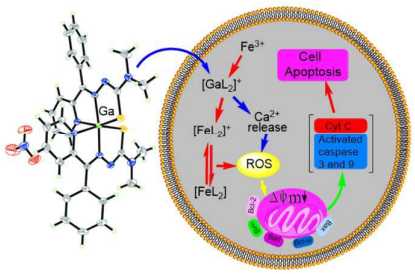

Ga (III) complexes promoted apoptosis as a result of a combination of multiple apoptotic pathways.